


 Cite this: *RSC Adv.*, 2022, **12**, 8536

# Crosslinked starch-coated cellulosic papers as alternative food-packaging materials

 Fatima-Zahra Semlali Aouragh Hassani,<sup>a</sup> Mohamed Hamid Salim,<sup>a</sup> Zineb Kassab,<sup>a</sup> Houssine Sehaqui,<sup>a</sup> El-Houssaine Ablouh,<sup>a</sup> Rachid Bouhfid,<sup>b</sup> Abou El Kacem Qaiss<sup>b</sup> and Mounir El Achaby<sup>a</sup>

In general, during the papermaking process or the production of cellulosic materials for food-packaging applications, lignin and other amorphous components are usually removed *via* the pulping and multilevel bleaching process to entirely separate them from the fiber. The aim of this work was to study the positive effect that can impart the residual lignin remaining in the alkali-treated fiber surface over bleached fibers to produce an alternative food-packaging cellulosic paper. Herein, cellulosic papers based on alkali-treated and bleached fibers obtained from the Alfa plant were successfully prepared using a compression process. The as-obtained papers were coated by crosslinked starch using a solvent-casting method to improve their mechanical and surface properties. The morphological and contact angle results showed that the residual lignin in the alkali-treated cellulosic papers strongly increased the interfacial adhesion by making the structure denser and more compact, resulting in an improved water resistance property over the bleached ones. On the other hand, it also promoted char formation, slowing down the burning process, resulting in better flame resistance. Additionally, the mechanical properties demonstrated that the presence of lignin contributed to the material rigidity improvement without compromising its flexibility (folding endurance). The as-developed cellulosic papers coated with crosslinked starch could be used for the production of high-quality materials for food-packaging applications using conventional industrial processes.

 Received 25th January 2022  
 Accepted 28th February 2022

DOI: 10.1039/d2ra00536k

[rsc.li/rsc-advances](http://rsc.li/rsc-advances)

## 1. Introduction

Due to the growing environmental awareness, there is a growing trend in the food-packaging industry to produce high-performance biodegradable materials made from natural resources.<sup>1–4</sup> The development of composites primarily made of natural fibers with a minor quantity of biopolymers has been a major goal in both academic and industrial research.<sup>1,2,5</sup> Natural fibers are also chosen because of their various advantages, such as being more cost-effective, environmentally friendly, and comparable mechanical properties to synthetic fibers.<sup>6–8</sup> However, their hydrophilic character leads to poor interfacial adherence with the matrix. Consequently, chemical treatment of the fiber's surface appears to be required.<sup>9–11</sup>

Bleaching treatment is the most commonly used process in the food-packaging industrial sector.<sup>6,12,13</sup> Indeed, the extracted cellulose is a natural fiber-derived product with excellent performance and customized mechanical and physical

qualities, making it the most appealing renewable material for sophisticated applications.<sup>6,14,15</sup> A major drawback associated with cellulose fibers is their hydrophilic nature causing their inability to disperse in non-polar fluids. Furthermore, processing such “pure” cellulosic materials is inefficient and usually comprises chemical treatment, bleaching, heat exchange, and separation stages (resource-intensive), resulting in significant cost increases.<sup>12,16</sup> Unlike the bleaching process, alkaline treatment is cost-effective and promotes only the partial removal of amorphous constituents, such as lignin, which is considered as the connecting material that holds the fibers together under hot compression, resulting in increased mechanical properties.<sup>17,18</sup> Also, it has been discovered that the presence of lignin has a good influence on the thermal and water resistance properties. Indeed, lignin contains aromatic rings that might promote flame retardancy, and it can tolerate high-temperature deterioration from 100 °C to 900 °C.<sup>6</sup> Besides, the inclusion of lignin-containing cellulosic fibers leads to more hydrophobic materials with a greater dispersion ability in non-polar media.<sup>17</sup>

However, the main issue with using chemically treated fibers alone are their low mechanical and water barrier properties. This can be avoided by employing a low quantity of biopolymers to coat the material's surface. Among the biopolymers, starch is one of the most promising renewable biopolymers because of

<sup>a</sup>Materials Science, Energy and Nanoengineering Department (MSN), Mohammed VI Polytechnic University (UM6P), Lot 660 – Hay Moulay Rachid, Benguerir, 43150, Morocco. E-mail: fatimazahra.semlali@um6p.ma; mounir.elachaby@um6p.ma

<sup>b</sup>Composites and Nanocomposites Center (CNC), Moroccan Foundation for Advanced Science, Innovation and Research (MAScIR), Rabat Design Center, Rue Mohamed El Jazouli, Madinat El Jfane, 10100 Rabat, Morocco



its versatility, low cost, abundance, and biodegradability.<sup>19,20</sup> Additionally, the mechanical, thermal and moisture protection properties of starch biopolymers can be further improved and adapted to meet specific needs by adding plasticizers and a crosslinking agent.<sup>21–23</sup> In fact, plasticizers, such as glycerol, allow the thermoplastic transformation of starch.<sup>23</sup> While the addition of a crosslinking agent, such as citric acid, improves the modulus, strength, thermal stability, water resistibility, and flammability resistance due to reducing the available OH groups of starch.<sup>24</sup> The most crucial aspect to remember is that glycerol and citric acid are nutritionally safe because they are nontoxic metabolic products of the body that have already been certified by the US FDA (Food and Drug Administration) for use in food compositions.<sup>25</sup>

In the same context, recent research in our laboratory investigated the effect of coating bleached date palm trays with chitosan modified with an antibacterial agent. The resulting coated material exhibited higher specific properties (morphological, mechanical, water resistance, and antimicrobial properties), making it suitable for the smart packaging industry.<sup>9</sup> Hassan *et al.*<sup>21</sup> investigated the effect of citric acid addition on the properties of starch/cellulose composite foams, and found that the addition of citric acid greatly improved the stiffness, flexural strength, and hydrophobicity of the material, which makes composite foams a good alternative to expanded polystyrene packaging. In contrast, Rosa *et al.*<sup>26</sup> studied the effect of three different chemical treatments (washing with water, alkaline treatment, and bleaching) of coir fibers on starch/EVOH/glycerol blends, using extrusion and injection processes. Chemical treatment was discovered to play a significant role in improving the material's mechanical properties, making it a great option for producing low-cost composites.

In this work the effect of chemical treatments was studied by investigating the effect of the residual lignin remaining in the alkali-treated fibers surface as compared to bleached ones in the production of high-performance food-packaging cellulosic paper. Thus, alkali-treated and bleached Alfa fibers were compression molded to produce cellulosic papers, and then coated with crosslinked starch (citric acid) using a solution-casting method. The effects of the residual lignin and starch crosslinked with acid citric on the morphological, mechanical, water resistance, and flame retardancy properties were evaluated.

## 2. Materials and methods

### 2.1. Materials

Potato starch with an average particle size of 45  $\mu\text{m}$  and a density of 1.49  $\text{g cm}^{-3}$  was isolated from fresh potato purchased at a local market in Benguerir, Morocco. The commercial starch used for the comparison was purchased from Sigma-Aldrich. The used raw Alfa fibers in this study were collected from the oriental region of eastern Morocco. The chemicals used for the fiber treatment were acetic acid ( $\text{CH}_3\text{-COOH}$ ), sodium hydroxide ( $\text{NaOH}$ ), and sodium chloride ( $\text{NaClO}_2$ ), and they were purchased from Sigma-Aldrich. All the materials were used without any further modification. Glycerol

was used as a plasticizer and citric acid as a crosslinking agent, both of them analytical reagent-grade and provided by Sigma-Aldrich.

### 2.2. Fiber preparation

Alfa fibers with an average initial length of 1000 mm were first chopped into 50–100 mm small fibers, then washed with tap water, air-dried for 24 h, ground in a knife mill (Retch SM100) with a screen size of 2 mm, and finally sieved through a 200  $\mu\text{m}$  opening to remove small particles.

### 2.3. Fiber surface modification

**2.3.1. Alkaline treatment.** Alkaline treatment was employed to eliminate the hemicellulose, lignin, and waxes from the Alfa fiber cell wall's exterior surface, as done in our previous works.<sup>9,10</sup> The fibers were immersed in an aqueous solution containing 6 wt% of  $\text{NaOH}$  for 18 h at room temperature, stirring constantly, before being filtered and rinsed with tap water.

**2.3.2. Bleaching process.** The alkali-treated fibers (AT-F) were bleached using a sodium chloride solution ( $\text{NaClO}_2$  at 1.7 wt%) in an acidic environment (pH 4–5) at 95 °C (oil bath) with continuous stirring for 5 h, as detailed in our previous works.<sup>9,10</sup> The mixture was then allowed to cool before being filtered, rinsed thoroughly with distilled water, and then oven dried at 60 °C, resulting in bleached cellulose fibers (BC-F).

### 2.4. Preparation of potato starch

First, 1 kg of potatoes was cleaned, peeled, and cut into small pieces to be mixed with distilled water using a blender. After that, the resulting slurry was run through a filter to remove any remaining water. The remaining solid mass was returned to the blender and the same amount of distilled water was added. The blending and filtering process was repeated five times to obtain the maximum starch possible. The mixture was left to stand in the beaker for 5 min. The supernatant liquid in the beaker was decanted, leaving the white starch that had sunk to the bottom. A quantity of distilled water was added to the starch and stirred gently. The process was repeated five times and then the water was decanted. The resulting starch was white in color as shown in Fig. 1. About 80 g of starch was obtained from 1 kg of potatoes, thus giving a yield of 8%.

### 2.5. Preparation of the coating solution

The potato starch biopolymer was prepared by adding 5 g of potato starch, 1.5 g of glycerol, and citric acid (CA) at two concentration (0 and 5 wt%) to distilled water (100 mL). The prepared two systems (with and without the crosslinking agent (CA)) were first stirred for 45 min at room temperature, and then heated at a rate of 3 °C per minute until reaching 90 °C. After that time, the mixtures remained under constant stirring for 5 min for complete starch gelatinization.



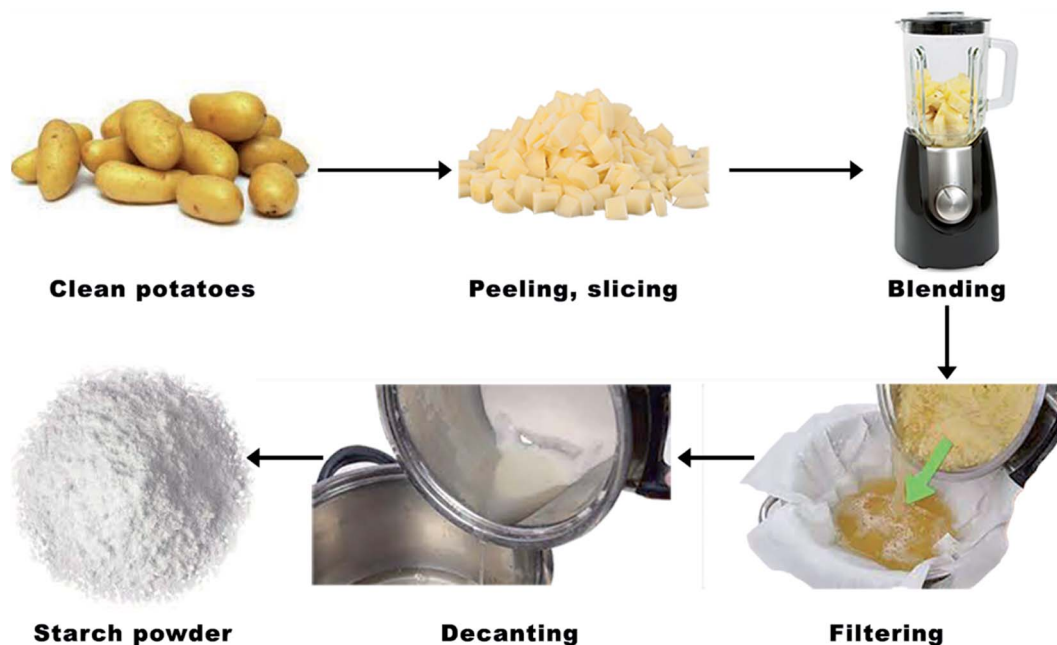


Fig. 1 Potato starch preparation.

## 2.6. Cellulosic papers preparation

For the cellulosic papers preparation, 2.5 g of the used fibers (AT-F and BC-F) was dispersed in water (100 mL) in order to be homogeneously layered on a circular mold (85 mm in diameter and 0.5 mm in thickness) to produce the two control materials: uncoated alkali-treated cellulosic papers (uc-ACP) and uncoated bleached cellulosic papers (uc-BCP). Then, the mold was compressed using a semi-automatic press (Carver Inc., USA) at 130 °C for 10 min to remove the water by evaporation and ensure a good bond of the fibers thanks to the lignin remaining on the fibers surface. Finally, the samples were removed from

the press, cooled for 15 min at room temperature, and demolded (Fig. 2).

The preparation of the other cellulosic papers was based on the solution-casting technique and the evaporation process. First, 18 g of the two biopolymer systems previously prepared (without and with citric acid) were poured into Petri dishes (90 mm in diameter), where uc-ACP and uc-BCP were impregnated, as illustrated in Fig. 2. This technique allows the materials to be coated with the biopolymers on both sides. After that, the mixtures (cellulosic papers impregnated in the biopolymer solutions) were oven dried at 45 °C overnight. Following the evaporation of the water, the resulting samples (coated on both

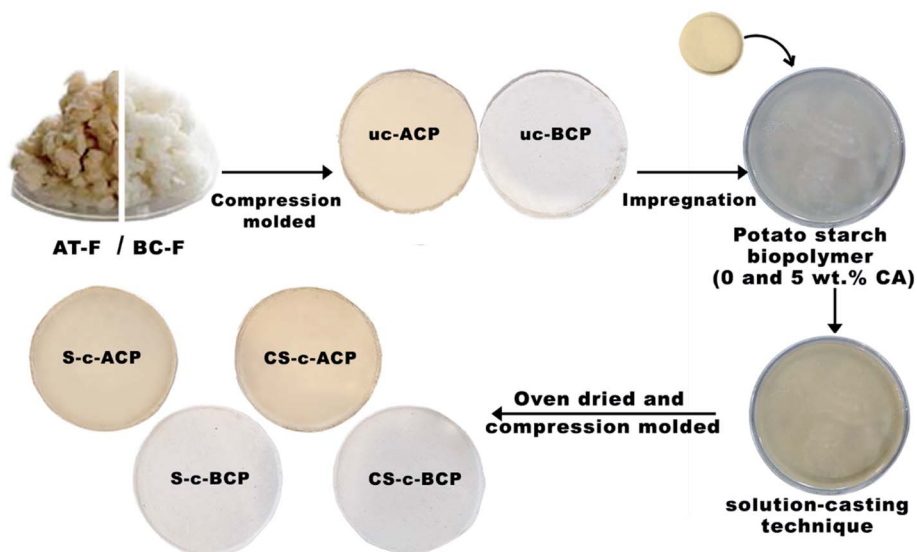


Fig. 2 Process of cellulosic papers preparation.



Table 1 The prepared cellulosic papers designations

Cellulosic papers category	Cellulosic papers designation	Fibers (g)	Starch (g)	Glycerol (g)	Citric acid (g) (5 wt%)
Alkali-treated	uc-ACP	2.5	—	—	—
	S-c-ACP	2.5	5	1.5	—
	CS-c-ACP	2.5	5	1.5	0,45
Bleached	uc-BCP	2.5	—	—	—
	S-c-BCP	2.5	5	1.5	—
	CS-c-BCP	2.5	5	1.5	0,45

sides) were removed, then compression molded a second time at 130 °C for 5 min to ensure the polymer homogenization and better fibers/matrix adhesion. Thus, the alkali-treated cellulosic papers coated with starch and crosslinked starch were denoted as “S-c-ACP” and “CS-c-ACP”, respectively, while the bleached cellulosic papers were denoted as “S-c-BCP” and “CS-c-BCP”, respectively, as explained in Table 1. It is to be well noted that all the materials were prepared using the same conditions for comparison purposes.

### 3. Characterization techniques

#### 3.1. X-Ray diffraction (XRD)

The crystalline structure of commercial starch and the extracted potato starch were identified and compared using a D8-Discover diffractometer from BRUKER. The samples were scanned in the  $2\theta$  range of 10°–40° with a step size of 0.01° using CuK $\alpha$  radiation ( $\lambda = 1.5418 \text{ \AA}$ ); the voltage and current were set at 40 KV and 100 mA, respectively.

#### 3.2. Fourier transform infrared spectroscopy (FTIR)

The FTIR spectra of the commercial and extracted potato starch, and the produced cellulosic papers were obtained on a PerkinElmer Spectrum 2000 equipped with an ATR accessory. Each spectrum was recorded in the range of 4000 to 600  $\text{cm}^{-1}$  and obtained by the accumulation of 16 consecutive scans with a resolution of 4  $\text{cm}^{-1}$ .

#### 3.3. Scanning electron microscopy (SEM)

The fracture surfaces of the control and coated cellulosic papers were examined by scanning electron microscopy (SEM, HIROX SH 4000M). Both surface and cross-section (samples were cut with a razor blade) images were made of the samples. Before imaging, the samples were coated with gold palladium in an ionization chamber to avoid charging under an accelerating voltage of 15 kV.

#### 3.4. Contact angle test

Contact angle (CA) analysis was used to determine the degree of surface hydrophobicity. This was performed at room temperature using an optical video contact angle device (OCA 40, Dataphysics, Germany) equipped with a charge-coupled-device camera and commercial image acquisition software (Scat). The CA was determined 10 s after dropping 10  $\mu\text{l}$  of water onto

the surface of the prepared cellulosic papers with a micro syringe. The average of three measurements was reported as a representative value.

#### 3.5. Cone calorimeter test

The flammability of the elaborated cellulosic papers was performed using a cone calorimeter device (Fire Testing Technology/Microcal) according to ISO 5660-1. Nearly 20 g of each material was exposed to a radiant cone at a heat flux of 35  $\text{kW m}^{-2}$ , corresponding to common heat flux in a mild fire scenario. The heat release rate (HRR) was measured as a function of time, and the time to ignition (TTI), total heat release (THR), peak heat release rate (pHRR), and effective heat of combustion (EHC) were determined.

#### 3.6. Tensile test

Tensile tests were performed at room temperature on a Universal Testing Machine Texture Analyzer (TA.XT plus) at a crosshead speed of 5  $\text{mm min}^{-1}$  using a 5 kN load cell and a gauge length of 30 mm, according to ISO 527-5. Thus the elaborated cellulosic papers were cut into  $10 \times 50 \times 0.5 \text{ mm}^3$  samples, and the average of five specimens was reported as a representative value.

#### 3.7. Dynamic mechanical analysis (DMA)

A dynamic mechanical analyzer (DMA 8000, PerkinElmer) was used to conduct the dynamic mechanical tests in the dual cantilever bending mode. Tests were conducted at a steady heating rate of 10 °C  $\text{min}^{-1}$  and frequency of 1 Hz to evaluate the storage modulus, loss modulus, and loss factor ( $\tan \delta$ ) as a function of temperature (10–150 °C). For the testing, the elaborated cellulosic papers were cut into  $10 \times 50 \times 0.5 \text{ mm}^3$  samples, and the average of five specimens was reported as a representative value.

## 4. Results and discussion

#### 4.1. X-Ray diffraction analysis

Starch is characterized by two main components: amylose, which is the linear structure that provides the crystalline structure of the starch, and amylopectin, which is the branched structure that presents the amorphous phase of the starch.<sup>27</sup> Fig. 3 shows the XRD patterns of the commercial potato starch and the extracted one. Both starches had similar strong





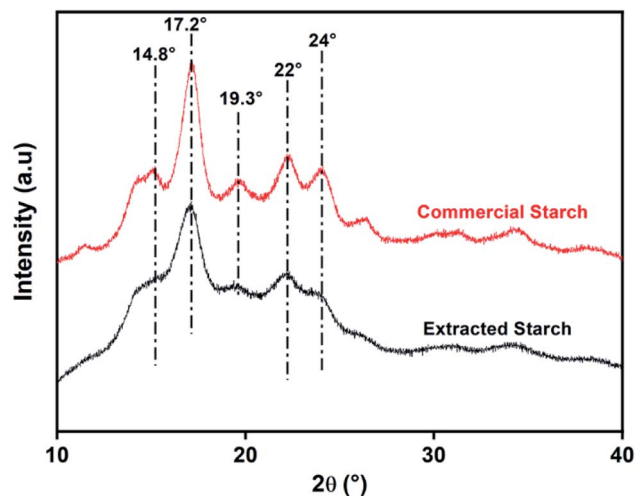


Fig. 3 XRD patterns of the commercial and extracted potato starches.

diffraction peaks, which were about  $17.2^\circ$ ,  $22^\circ$ , and  $24^\circ$ , as well as weak diffraction peaks around  $14.8^\circ$  and  $19.3^\circ$ . These peaks indicated that both potato starches had a B-type crystalline structure<sup>28</sup> (hexagonal symmetry, with the space group P61 (ref. 29)). The only difference observed between the commercial and extracted potato starches was a slight decrease in the diffraction peaks' intensity for the extracted potato starch, and this can be explained by the difference in crystallinity caused by differences in the water content and/or the temperature used during the extraction method.<sup>30</sup>

#### 4.2. Fourier transform infrared spectroscopy analysis

FTIR spectroscopy analysis is regarded a valuable tool to evaluate changes in the starch structure at a molecular level (short-range order), such as starch chain conformation, helicity, crystallinity, and retrogradation phases.<sup>31</sup> This was first performed to identify the extracted starch's key functional groups and to confirm the structure of the starches.<sup>32</sup> FTIR spectra of the starches also revealed peaks originating primarily from the vibrational modes of the starch components, including amylose

and amylopectin molecules.<sup>32</sup> For this, the FTIR spectra of the extracted and commercial starch were compared and the results are presented in Fig. 4a. By comparing the two spectra, it is evident that they showed almost similar forms and peaks, implying that they have similar chemical structures.<sup>31</sup> The peaks around  $3325$  and  $2920\text{ cm}^{-1}$  represented, respectively, the stretching vibration of  $-\text{OH}$  and  $-\text{CH}$  groups, while the peak  $1642\text{ cm}^{-1}$  was assigned to the  $\text{H}-\text{O}-\text{H}$  bending vibration of water molecules.<sup>32</sup> Furthermore, the peaks that emerged at  $1426$  and  $1334\text{ cm}^{-1}$  depicted, respectively, the angular twisting of  $\text{C}-\text{H}$  and  $\text{CH}_2$ .<sup>32</sup> The strong peaks near  $1156$ ,  $1080$ , and  $1010\text{ cm}^{-1}$  indicated, respectively, the stretching vibration of  $\text{C}-\text{O}-\text{C}$  and  $\text{C}-\text{O}-\text{H}$  from glycosidic bonds, which are characteristic of polysaccharides.<sup>32,33</sup> Finally, the skeletal mode vibration of the-1,4 glycosidic linkage was ascribed to the peaks about  $925\text{ cm}^{-1}$ .<sup>32,33</sup> However, differences in intensity were observed, which may be due to the different water contents and crystallinities of the starches resulting from the extraction method, as evidenced by the XRD analysis.<sup>34</sup>

Fig. 4b presents the IR spectra for the alkali-treated and bleached cellulosic papers. The main peaks around  $3200\text{--}3600\text{ cm}^{-1}$  exhibited the absorption bands characteristic of the  $\text{O}-\text{H}$  stretching vibration and  $\text{C}-\text{O}$  groups of cellulose.<sup>10,35</sup> The bands at  $2850$  and  $2923\text{ cm}^{-1}$  were assigned to symmetric and asymmetric  $\text{C}-\text{H}$  stretching vibrations.<sup>21</sup> The lack of the peak at  $1250\text{ cm}^{-1}$  for the bleached cellulosic papers demonstrated that the lignins, pectins, waxes, and hemicelluloses were completely removed from the fiber surface during the bleaching procedure.<sup>10</sup> The organized and amorphous starch structures were attributed to the three characteristic bands at  $1080$ ,  $1014$ , and  $960\text{ cm}^{-1}$ , assigned to the  $\text{C}-\text{O}$  bond stretching band, confirming that the starch powder extracted from potato corresponded to the commercial starch powder.<sup>21,23</sup> The changes observed in the infrared absorption band around  $1150\text{ cm}^{-1}$  were attributed to the  $\text{C}-\text{O}-\text{C}$  asymmetric stretching vibrations, and were associated with changes in the glycosidic bonds in the starch molecules, leading to a decrease in hydrophilicity.<sup>21,23</sup> In addition, the emergence of a new absorption band at  $1724\text{ cm}^{-1}$ , characteristic of carbonyls such as carboxylic acids and esters, confirmed the chemical linkages between the

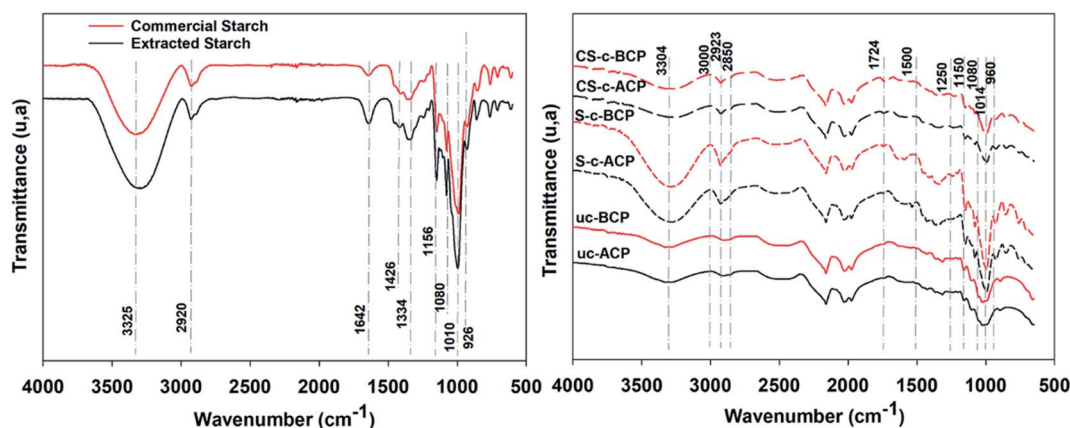


Fig. 4 FTIR spectra of the starches and elaborated cellulosic papers.



carboxyl groups of the citric acid and the free hydroxyl groups of the starch and belonged to C–O stretching.<sup>36,37</sup> While in the crosslinked composites, the drops in the band intensities for the hydroxyl groups around  $3000\text{ cm}^{-1}$  and the bound water molecules around  $1500\text{ cm}^{-1}$  were due to the rearrangements and formation of new hydrogen bonds.<sup>36</sup>

### 4.3. Morphological analysis

The state of the fiber-crosslinked starch interface adhesion is crucial in determining the performance of the elaborated cellulosic papers. To understand the compatibility between the alkali-treated or bleached Alfa fibers and the crosslinked potato starch biopolymer by citric acid, a top-view and a cut-out edge view of all the cellulosic papers were evaluated using SEM analysis. From Fig. 5, it can be clearly seen that the uncoated alkali-treated cellulosic papers (uc-ACP) exhibited fibers strongly bonded to each other with an almost continuous surface under only hot compression, compared to the bleached ones (uc-BCP). Indeed, the bleaching process caused a total or partial fibrillation and cleaned the fiber surface of a great amount of impurities, such as lignin, which are responsible for the fibers sticking.<sup>9,26</sup> Coating the cellulosic papers with starch polymer resulted in better interfacial adhesion, while it was clear that the cellulose/starch cellulosic papers showed quite different morphologies compared to the citric acid-crosslinked ones.

For the non-crosslinked starch cellulosic papers (S-c-ACP and S-c-BCP), cellulosic fibers were visible on the surface, especially for the bleached ones, because the fibers did not create a strong binding with the starch biopolymer. While with the addition of citric acid, the spreading of starch increased, resulting in gelatinized starch particles on the crosslinked cellulosic papers surface (CS-c-ACP and CS-c-BCP). Indeed, citric acid is very hygroscopic and binds water molecules, slowing moisture evaporation during high-temperature crosslinking, allowing starch particles to fully gelatinize and spread, which explains the smoother surface of the crosslinked papers.<sup>21</sup>

In order to further investigate the fibers dispersion/distribution state and the effect of crosslinking, cross-sections of the elaborated cellulosic papers were also analyzed. Fig. 6 exhibits clearly a poor interfacial adhesion in the bleached cellulosic papers, resulting in a sandwich-type structure upon the polymer addition. Furthermore, the acid citric addition did not enhance as much as expected the bleached fiber/biopolymer compatibility. Unlike the expanded structure of the sandwich center layer, the outer layers had a nearly denser structure, and therefore less voids, which explains the smoother surface observed in Fig. 5. This type of structure is generally common when the compression process is used. Water vapor expands the material, forming cells that are larger in the center and smaller at the ends, where the dense layer forms.<sup>36,38</sup> Despite using the same process, the alkali-treated cellulosic papers presented a better interfacial adhesion. Additionally, adding the acid citric to the alkali-treated fibers (CS-c-ACP) resulted in a more dense and compact structure. This change could be explained by the decreased chain mobility in the crosslinked starch chains that resulted in an improved interfacial adhesion, a decreased expansion of the material, and thus in an increase in the cellulosic papers mechanical properties.<sup>36,38</sup>

### 4.4. Contact angle analysis

The susceptibility of starch-based materials to moisture and water is one of their key disadvantages. As a result, a water resistance test was performed using contact angle analysis to see how the cellulosic papers behaved when exposed to water. According to the literature, the higher the contact angle value, the higher the material's hydrophobicity and *vice versa*.<sup>9,39</sup> As shown in Fig. 7, coating the control alkaline and bleached cellulosic papers with starch polymer resulted in better water resistance, which can be explained by the strong interaction between the starch and fibers.<sup>25,40</sup> The hydrogen connections between them did indeed inhibit water's interaction with the cellulosic papers.<sup>25,40</sup> In addition, adding the crosslinking agent

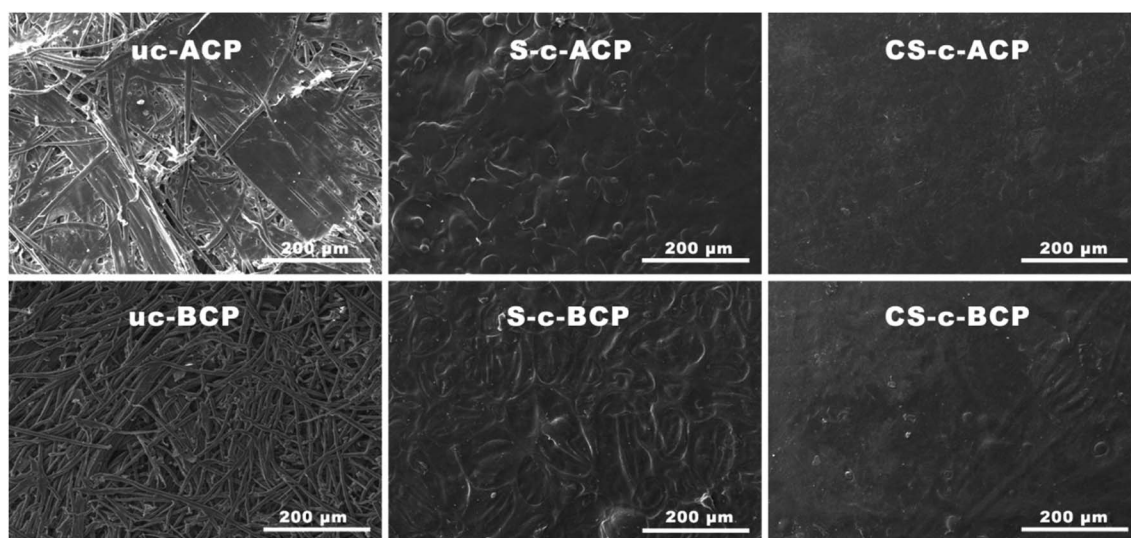


Fig. 5 SEM micrographs of the elaborated cellulosic papers surface.



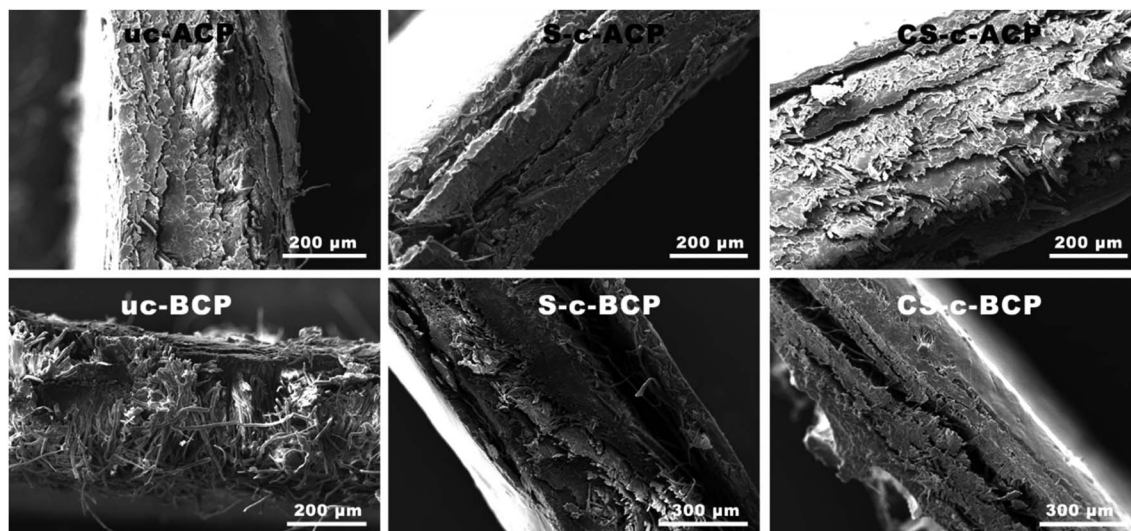


Fig. 6 SEM micrographs of the elaborated cellulosic papers cross-sections.

significantly increased the contact angle value for the alkali-treated and bleached cellulosic papers, respectively, by 70% and 55%, when compared to the control ones. This was due to the strong interfacial adhesion given by the citric acid cross-linking agent, as evidenced by the SEM results detailed above. On the other hand, due to the production of hydrophobic ester groups between citric acid and the polysaccharides, as revealed by FTIR analysis, this resulted in a reduction in the number of polar groups, preventing water absorption from the composites surface.<sup>41</sup> The fact that the crosslinked alkali-treated cellulosic papers had better hydrophobicity ( $114.60^\circ \pm 1.09$ ) than the bleached ones ( $92.37^\circ \pm 1.56$ ) was due to the lignin content, as previously stated. Indeed, in addition of the citric acid effect, lignin acted as a cementing material between the fibrils, resulting in a more dense and compact structure and thus making the structure resistant against water absorbance.<sup>42,43</sup>

#### 4.5. Flame retardancy analysis

The peak heat release rate (pHRR) and total heat release (THR) are two key factors for determining a material's flammability.<sup>44</sup> Generally, the kind of chemical treatment has a significant impact on the flame retardant qualities of composites derived from natural fibers. Natural fibers, which are made up of cellulose, hemicellulose, lignin, waxes, and pectin, are thought to act as combustion sources in composites. In comparison to alkaline treatment, bleaching those fibers is known to clean the fibers surface of a huge quantity of impurities, such as lignin.<sup>9,10</sup> It is commonly known that weak bonds break at a lower temperature in lignin, but strong linkages, such as the C-C linkage and other aromatic rings, dissociate at a greater temperature. The presence of lignin affects cellulose breakdown by accelerating dehydration and enhancing the development of char.<sup>45</sup> Char formation is important for assessing the

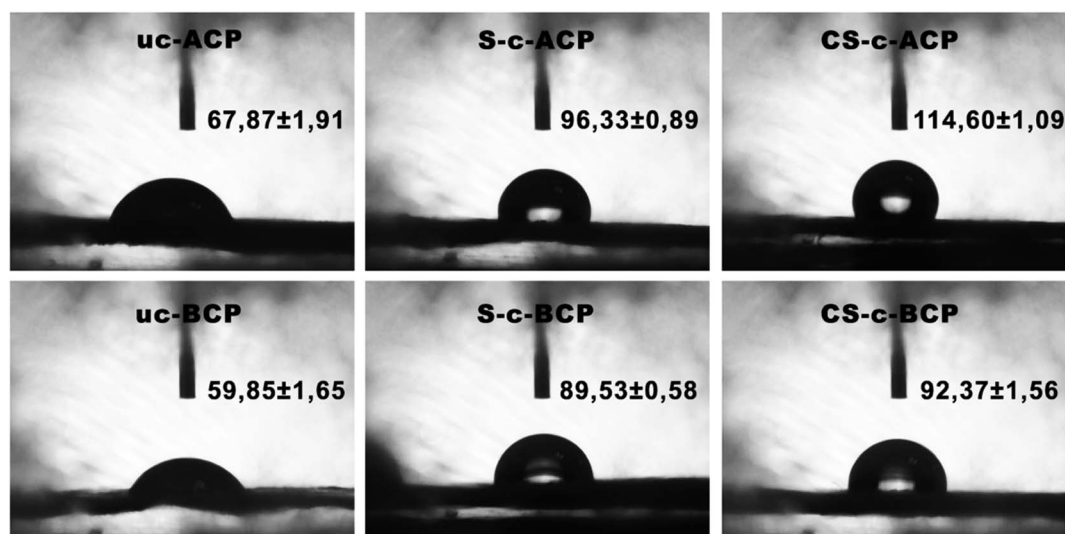


Fig. 7 Contact angle of the elaborated cellulosic papers.





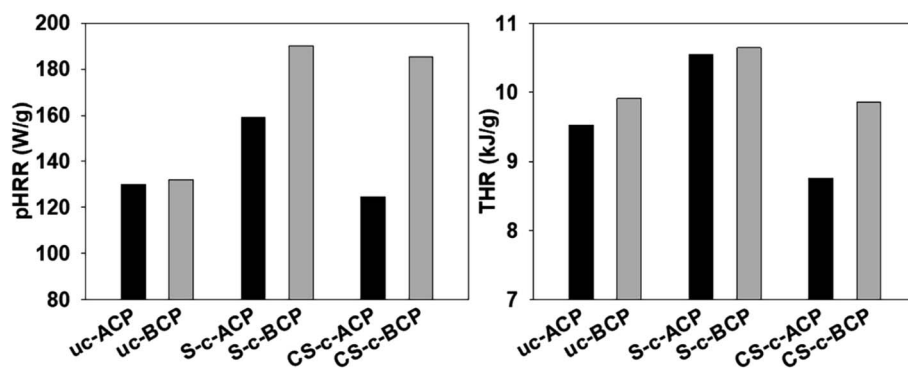


Fig. 8 Peak heat release rate (pHRR) and total heat release (THR) of the elaborated cellulosic papers.

flammability qualities because it increases flame retardancy, protects the underlying substrate from further deterioration, and slows down the burning rate, which explain why pHRR and THR were lower in the alkaline treatment systems than in the bleached ones (Fig. 8).<sup>6</sup> The presence of citric acid in the crosslinked cellulosic papers (CS-c-ACP and CS-c-BCP) increased the fibers/starch biopolymer interfacial adhesion, decreasing the flow-ability of starch and minimizing the dripping effect of the cellulosic papers, thus improving the fire retardancy. Also, as shown in the SEM images, the better distribution and dispersion of Alfa fibers in the alkali-treated cellulosic papers helped to create a barrier between the

burned and unburned materials, inhibiting fire growth and lowering the amount of volatiles and oxygen in the fire zone, resulting in the better flame retardancy results.<sup>6</sup>

#### 4.6. Tensile analysis

The effect of the fiber treatments and crosslinking agent on the developed cellulosic papers is illustrated in Fig. 9, where it is obvious that the alkali-treated cellulosic papers had better tensile properties than the bleached ones. According to Fig. 9a and b, adding potato starch to the alkali-treated and bleached cellulosic papers had a positive effect on both the Young's modulus and tensile strength, which can be explained by the

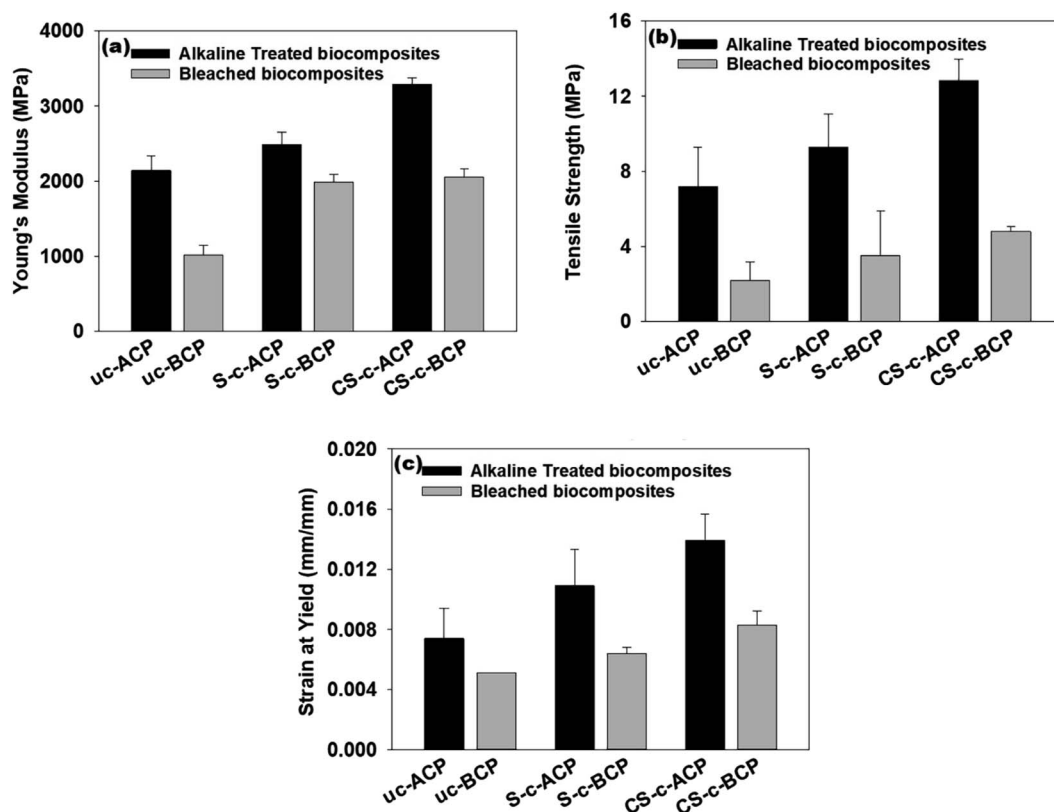


Fig. 9 Tensile properties of the elaborated cellulosic papers.





improved interfacial adhesion.<sup>9,46,47</sup> In comparison to the control cellulosic papers, crosslinking starch cellulosic papers with citric acid increased the Young's modulus by more than 103% and the tensile strength by more than 120%. Indeed, crosslinking joined the starch molecules in the cellulosic papers, thus increasing the starch's molecular weight while also improving the intermolecular interactions, resulting in higher interfacial adhesion and hence a better tensile modulus and tensile strength.<sup>37,48,49</sup> The mechanical properties are not only linked to the crosslinker, but also to the plasticizer. Generally, adding a crosslinker and plasticizer to composites improves the tensile strength and drops the strain at yield.<sup>25,50</sup> In our case, the addition of citric acid increased noticeably both the material strength and elongation by more than 88%, which were also due to the inherent strong fiber/biopolymer interaction (Fig. 9c).<sup>22</sup> The fact that the alkali-treated cellulosic papers presented a higher mechanical performance than the bleached ones, in this case, was due to the amount of fibers lignin content. As illustrated in the SEM images, lignin is responsible for the fibers sticking and thus in improving the interfacial adhesion.<sup>9,12</sup> To deduce that, producing cellulosic papers with alkali-treated fibers is a good alternative, as it allows a strong improvement in the flexibility without sacrificing the strength.

#### 4.7. Dynamic mechanical analysis (DMA)

DMA was used to determine the thermomechanical characteristics of the elaborated cellulosic papers. Most polymer samples do not have the same properties at different temperatures. As our materials are dedicated to the food-packaging sector, the test was carried out in a temperature range between 10 °C and 150 °C to understand the mechanical behavior of cellulosic papers when subjected to this temperature range rather than room temperature. The storage modulus  $E'$  is a measure of a composite's ability to store mechanical energy upon reversible elastic deformation; the higher the storage modulus, the stiffer the material.<sup>51,52</sup> The dependency of the elaborated cellulosic papers storage modulus on the temperature is shown in Fig. 10a. This dependency is due to the thermal transitions associated with amorphous components, demonstrating the usual viscoelasticity of the papers manufactured from cellulose fibers.<sup>53</sup> Indeed as the temperature increased, the values of the storage modulus decreased until approximately 20 °C for the uncoated cellulosic papers, and until 40 °C for the coated ones, indicating an increase in molecular mobility.<sup>53,54</sup> Beyond this temperature, an increase in  $E'$  was noticed until reaching approximately 120 °C, ascribed to the water evaporation, which acted as a plasticizer and adhered to the cellulose papers.<sup>51,53</sup> When a large amount of water was evaporated, the storage modulus declined again as the temperature rose.<sup>54</sup> By comparing the alkali-treated and bleached cellulosic papers, it is clear that the chemical treatments had a considerable impact on the composite's stiffness and flexibility. For the bleached cellulosic papers, coating the uc-BCPs with non-crosslinked starch biopolymer slightly increased the storage modulus, while crosslinking starch using citric acid was found to strongly increase the material rigidity over the entire range of the studied temperatures, which was in good agreement with the

tensile test assays referred to before. Crosslinking does indeed join the starch molecules in cellulosic papers, restricting the mobility of the polymer chains, resulting in higher stiffness and a loss of flexibility.<sup>55–57</sup> Here, the higher storage modulus (stiffness) of the alkali-treated cellulosic papers than the bleached ones was attributed to the better interfacial adhesion, as evidenced by the SEM images.<sup>58</sup> However, coating the alkali-treated cellulosic papers seemed to lead to an opposite behavior, since it decreased the storage modulus over the entire range of temperature. This decrease in storage modulus corresponded to more molecular mobility while preserving better flexibility, and thus a higher folding endurance.<sup>53,57</sup> The flexibility is another important parameter to consider for cellulosic papers, since it indicates an improved durability of the cellulosic papers.<sup>59</sup> As expected, the quantity of lignin content remaining in the alkali-treated fibers strongly improved the interfacial adhesion. On the other hand, the addition of the crosslinked starch contributed to a greater improvement of the intermolecular interactions, resulting in better flexibility without sacrificing the strength, which was in good agreement with the tensile and SEM results.<sup>9,12</sup>

The loss factor ( $\tan \delta$ ) is the ratio of energy loss to energy stored per cycle deformation and its peak represents the glass transition temperature.<sup>60</sup> In other words, it gives information on how well a material absorbs energy.<sup>60</sup> Fig. 10b presents  $\tan \delta$  of the elaborated cellulosic papers as a function of temperature.

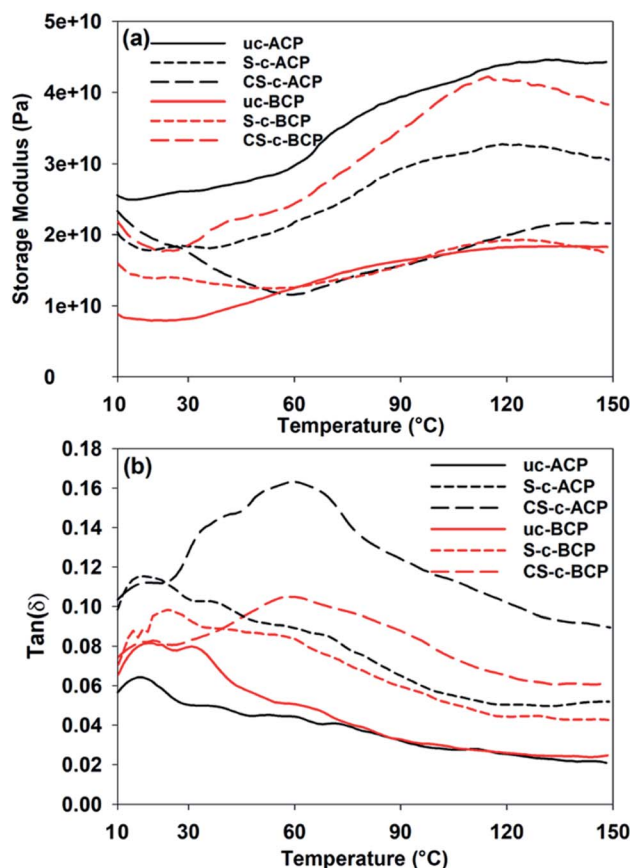


Fig. 10 Dynamic mechanical analysis of the elaborated cellulosic papers.



Marica *et al.*<sup>61</sup> reported a similar trend of  $\tan \delta$  for cellulosic papers from different plants, reporting that the viscoelastic behavior of cellulosic papers can be mainly attributed to the lignin and hemicellulose.<sup>61</sup> It is also important to emphasize that the temperature relaxation behavior of the cellulose structure is extremely complex due to its heterogeneity, so it is difficult to distinguish which component is responsible for the overall behavior of the structure.<sup>61</sup> Consequently, the structural mobility of hemicellulose and lignin under the impact of ambient heat and moisture is ascribed to the relaxation region reported between 10 °C and 50 °C for cellulosic papers.<sup>61</sup> Here, the relaxation transition at approximately 60 °C for the starch-coated composites was associated with the glass transition of the starch-rich phase,<sup>22,62</sup> whereas the addition of citric acid shifted the relaxation peak of starch toward higher temperature (60–90 °C). This discovery confirmed the strong interfacial adhesion between the fibers and crosslinked starch, as well as the improved thermal stability of cellulosic papers, as evidenced by the flame resistance analysis.<sup>62</sup> Additionally, the addition of the starch polymer and crosslinking agent increased the loss factor by 108% for the bleached cellulosic papers and 275% for the alkali-treated cellulosic papers at 60 °C, indicating a greater energy dissipation.<sup>60,63</sup> It can also be seen from Fig. 10b that the alkali-treated cellulosic fibers had a loss factor higher than the bleached ones. This finding could be explained by the residual lignin on the alkali-treated fibers' surface, which acted as a compatibilizer and improved the materials flexibility.<sup>2,61</sup>

## 5. Conclusion

Sustainable food-packaging papers based on Alfa plant-derived alkali-treated and bleached cellulosic fibers were successfully prepared using a compression process. The as-prepared papers were coated by a crosslinked starch biopolymer, using solution-casting technology, to improve their surface hydrophobicity and mechanical properties as well as their morphological features. Coating the alkaline-treated cellulosic papers with crosslinked starch was found to give better results than for the bleached ones. Indeed, the residual lignin in the alkali-treated fiber's surface was responsible for the fibers sticking and thus in showing better interfacial adhesion. As evidenced by the contact angle results, CS-c-ACP demonstrated a 25% greater water resistance than CS-c-BCP. Also from the flame cone calorimeter tests, it was found that the lignin enhanced the development of char, which led to a considerable increase in flame resistance. In terms of the mechanical properties, the tensile tests showed that the use of alkali-treated fibers exhibited a Young's modulus, tensile strength, and elongation 60%, 170%, and 68% better than the bleached ones, respectively. Whereas the dynamic mechanical analysis revealed that the remaining residual lignin in the fibers surface increased the materials flexibility (folding endurance) without compromising their rigidity. To conclude, the suggested as-developed cellulosic papers coated with crosslinked starch could be used to produce food-packaging materials with enhanced water resistance, flame retardancy, and mechanical properties.

## Conflicts of interest

The authors declare that they have no known competing financial interests. The manuscript has not been published elsewhere and that it has not been submitted simultaneously for publication elsewhere.

## Acknowledgements

The financial assistance of the Office Chérifien des Phosphates (OCP S.A.) in the Moroccan Kingdom toward this research is hereby acknowledged.

## References

- 1 P. Baishya, D. Saikia, M. Mandal and T. K. Maji, *Polym. Compos.*, 2019, **40**, 46–55.
- 2 L. Zhang, Z. Li, Y. T. Pan, A. P. Yáñez, S. Hu, X. Q. Zhang, R. Wang and D. Y. Wang, *Composites, Part B*, 2018, **154**, 56–63.
- 3 K. El Bourakadi, F. Semlali Aouragh Hassani, A. E. K. Qaiss and R. Bouhfid, in *Biopolymers and Biocomposites from Agro-Waste for Packaging Applications*, ed. Naheed Saba, Mohammad Jawaid and Mohamed Thariq, Elsevier, 1st edn, 2021, pp. 35–63.
- 4 C. M. O. Müller, J. B. Laurindo and F. Yamashita, *Food Hydrocolloids*, 2009, **23**, 1328–1333.
- 5 F. Semlali Aouragh Hassani, W. Ouarhim, N. Zari, R. Bouhfid and A. Qaiss, in *Biodegradable Composites Materials, Manufacturing and Engineering*, ed. K. Kumar and J. P. Davim, De Gruyter, 1st edn, 2019, pp. 49–79.
- 6 F. A. Sabaruddin, P. M. Tahir, S. M. Sapuan, R. A. Ilyas, S. H. Lee, K. Abdan, N. Mazlan, A. S. M. Roseley and A. Khalil Hps, *Polymers*, 2021, **13**, 1–19.
- 7 F. Semlali Aouragh Hassani, W. Ouarhim, Z. Kassab, M. E. L. Achaby, R. Bouhfid and A. Qaiss, in *Cellulose Nanoparticles: Volume 2*, ed. Vijay Kumar Thakur, Elisabete Frollini and Janet Scott, Synthesis and Manufacturing, 2021, pp. 298–322.
- 8 D. Liu, T. Zhong, P. R. Chang, K. Li and Q. Wu, *Bioresour. Technol.*, 2010, **101**, 2529–2536.
- 9 F. Semlali Aouragh Hassani, K. El Bourakadi, N. Merghoub, A. el kacem Qaiss and R. Bouhfid, *Int. J. Biol. Macromol.*, 2020, **148**, 316–323.
- 10 F. Semlali Aouragh Hassani, W. Ouarhim, M. Raji, M. E. M. Mekhzoum, M. O. Bensalah, H. Essabir, D. Rodrigue, R. Bouhfid and A. el kacem Qaiss, *J. Polym. Environ.*, 2019, **27**, 2974–2987.
- 11 M. Kamali, T. Gameiro, M. E. V. Costa and I. Capela, *Chem. Eng. J.*, 2016, **298**, 162–182.
- 12 K. L. Spence, R. A. Venditti, Y. Habibi, O. J. Rojas and J. J. Pawlak, *Bioresour. Technol.*, 2010, **101**, 5961–5968.
- 13 R. Mu, X. Hong, Y. Ni, Y. Li, J. Pang, Q. Wang, J. Xiao and Y. Zheng, *Trends Food Sci. Technol.*, 2019, **93**, 136–144.
- 14 J. Behin and M. Zeyghami, *Chem. Eng. J.*, 2009, **152**, 26–35.



- 15 S. Guzman-Puyol, L. Ceseracciu, J. A. Heredia-Guerrero, G. C. Anyfantis, R. Cingolani, A. Athanassiou and I. S. Bayer, *Chem. Eng. J.*, 2015, **277**, 242–251.
- 16 F. Semlali Aouragh Hassani, H. Chakchak, M. El Achaby, R. Bouhfid and A. E. K. Qaiss, in *Date Palm Fiber Composites: Processing, Properties and Applications*, ed. Mohamad Midani, Naheed Saba and Othman Y. Alothman, Springer, 1st edn, 2020, pp. 75–91.
- 17 K. C. C. Carvalho, D. R. Mulinari, H. J. C. Voorwald and M. O. H. Cioffi, *BioResources*, 2010, **5**, 1143–1155.
- 18 M. Shahbazi, S. J. Ahmadi, A. Seif and G. Rajabzadeh, *Food Hydrocolloids*, 2016, **61**, 378–389.
- 19 J. Guan and M. A. Hanna, *Bioresour. Technol.*, 2006, **97**, 1716–1726.
- 20 C. Herniou-Julien, J. R. Mendieta and T. J. Gutiérrez, *Food Hydrocolloids*, 2019, **89**, 67–79.
- 21 M. M. Hassan, N. Tucker and M. J. Le Guen, *Carbohydr. Polym.*, 2020, **230**, 115675.
- 22 H. Kargarzadeh, N. Johar and I. Ahmad, *Compos. Sci. Technol.*, 2017, **151**, 147–155.
- 23 K. Jeyasubramanian and R. Balachander, *Journal of Achievements in Materials and Manufacturing Engineering*, 2016, **75**, 78–84.
- 24 M. J. Tavera-Quiroz, J. Ferial Díaz and A. Pinotti, *Int. J. Appl. Eng. Res.*, 2018, **13**, 13302–13307.
- 25 B. Ghanbarzadeh, H. Almasi and A. A. Entezami, *Ind. Crops Prod.*, 2011, **33**, 229–235.
- 26 M. F. Rosa, B. sen Chiou, E. S. Medeiros, D. F. Wood, T. G. Williams, L. H. C. Mattoso, W. J. Orts and S. H. Imam, *Bioresour. Technol.*, 2009, **100**, 5196–5202.
- 27 M. Todica, E. M. Nagy, C. Niculaescu, O. Stan, N. Cioica and C. V. Pop, *J. Spectrosc.*, 2016, **2016**, 1–6.
- 28 K. Kalantari, A. M. Affi, H. Jahangirian and T. J. Webster, *Carbohydr. Polym.*, 2019, **207**, 588–600.
- 29 D. R. Barros, A. P. M. G. Carvalho, E. O. da Silva, U. M. Sampaio, S. M. de Souza, E. A. Sanches, A. de Souza Sant'Ana, M. T. P. S. Clerici and P. H. Campelo, *Int. J. Biol. Macromol.*, 2021, **168**, 187–194.
- 30 S. Jagadeesan, I. Govindaraju and N. Mazumder, *Am. J. Potato Res.*, 2020, **97**, 464–476.
- 31 R. Singh, S. Kaur and P. A. Sachdev, *Journal of Food Measurement and Characterization*, 2021, **15**, 3168–3181.
- 32 M. Deng, C. K. Reddy and B. Xu, *Int. J. Biol. Macromol.*, 2020, **158**, 648–655.
- 33 A. M. Pascoal, M. C. B. Di-Medeiros, K. A. Batista, M. I. G. Leles, L. M. Lião and K. F. Fernandes, *Carbohydr. Polym.*, 2013, **98**, 1304–1310.
- 34 M. M. Andrade-Mahecha, D. R. Tapia-Blácido and F. C. Menegalli, *Starch/Staerke*, 2012, **64**, 348–358.
- 35 L. Costes, F. Laoutid, F. Khelifa, G. Rose, S. Brohez, C. Delvosalle and P. Dubois, *Eur. Polym. J.*, 2016, **74**, 218–228.
- 36 K. Pornsuksomboon, B. B. Holló, K. M. Szécsényi and K. Kaewtatip, *Carbohydr. Polym.*, 2016, **136**, 107–112.
- 37 A. Sonia, K. Priya Dasan and R. Alex, *Chem. Eng. J.*, 2013, **228**, 1214–1222.
- 38 B. F. Bergel, S. D. Osorio, L. Machado, R. Marlene and C. Santana, *Carbohydr. Polym.*, 2018, **200**, 106–114.
- 39 Y. Pan, F. Wang, T. Wei, C. Zhang and H. Xiao, *Chem. Eng. J.*, 2016, **302**, 33–43.
- 40 M. Li, X. Tian, R. Jin and D. Li, *Ind. Crops Prod.*, 2018, **123**, 654–660.
- 41 H. Wu, Y. Lei, J. Lu, R. Zhu, D. Xiao, C. Jiao, R. Xia, Z. Zhang, G. Shen, Y. Liu, S. Li and M. Li, *Food Hydrocolloids*, 2019, **97**, 105208.
- 42 M. Hassan, L. Berglund, E. Hassan, R. Abou-Zeid and K. Oksman, *Cellulose*, 2018, **25**, 2939–2953.
- 43 S. M. Davachi, S. Bakhtiari, P. Pouresmael-Selakjani, J. Mohammadi-Rovshandeh, B. Kaffashi, S. Davoodi and A. Yousefi, *Adv. Polym. Technol.*, 2018, **37**, 5–16.
- 44 X. Yang and W. Zhang, *Flame retardancy of wood-polymeric composites*, Elsevier Inc., 2018.
- 45 M. Rashid, K. Chetehouna, A. Cablé and N. Gascoin, *Analysing Flammability Characteristics of Green Biocomposites: An Overview*, 2021, vol. 57.
- 46 A. R. Kakroodi, Y. Kazemi, M. Nofar and C. B. Park, *Chem. Eng. J.*, 2017, **308**, 772–782.
- 47 A. M. Salaberria, J. Labidi and S. C. M. Fernandes, *Chem. Eng. J.*, 2014, **256**, 356–364.
- 48 N. Reddy and Y. Yang, *Food Chem.*, 2010, **118**, 702–711.
- 49 E. D. R. Zavareze, V. Z. Pinto, B. Klein, S. L. M. El Halal, M. C. Elias, C. Prentice-Hernández and A. R. G. Dias, *Food Chem.*, 2012, **132**, 344–350.
- 50 R. Shi, J. Bi, Z. Zhang, A. Zhu, D. Chen, X. Zhou, L. Zhang and W. Tian, *Carbohydr. Polym.*, 2008, **74**, 763–770.
- 51 S. Rat, V. Nagy, I. Suleimanov, G. Molnár, L. Salmon, P. Demont, L. Csóka and A. Bousseksou, *Chem. Commun.*, 2016, **52**, 11267–11269.
- 52 X. Ma, M. Lv, D. P. Anderson and P. R. Chang, *Food Hydrocolloids*, 2017, **66**, 276–285.
- 53 Z. Li, W. Liu, F. Guan, G. Li, Z. Song, D. Yu, H. Wang and H. Liu, *Carbohydr. Polym.*, 2019, **214**, 26–33.
- 54 X. Ma, R. Jian, P. R. Chang and J. Yu, *Biomacromolecules*, 2008, **9**, 3314–3320.
- 55 P. Balakrishnan, M. S. Sreekala, M. Kunaver, M. Huskić and S. Thomas, *Carbohydr. Polym.*, 2017, **169**, 176–188.
- 56 P. Guerrero, A. Muxika, I. Zarandona and K. de la Caba, *Carbohydr. Polym.*, 2019, **206**, 820–826.
- 57 G. G. Xu and C. Q. X. Yang, *J. Appl. Polym. Sci.*, 1999, **74**, 907–912.
- 58 P. Balakrishnan, S. Gopi, V. G. Geethamma, N. Kalarikkal and S. Thomas, *Macromol. Symp.*, 2018, **380**, 1–7.
- 59 M. Karlovits and D. Gregor-Svetec, *Acta Polytechnica Hungarica*, 2012, **9**, 81–100.
- 60 P. Baishya and T. K. Maji, *Cellulose*, 2017, **24**, 4263–4274.
- 61 M. Starešinič, B. Boh Podgornik, D. Javoršek, M. Leskovšek and K. Možina, *Forests*, 2021, **12**, 527–553.
- 62 N. Soykeabkaew, N. Laosat, A. Ngaokla, N. Yodsuwan and T. Tunkasiri, *Compos. Sci. Technol.*, 2012, **72**, 845–852.
- 63 A. Jabbar, J. Militký, J. Wiener, B. M. Kale, U. Ali and S. Rwawiire, *Compos. Struct.*, 2017, **161**, 340–349.

